Diabetes mellitus and tuberculosis comorbidity induce unique microbial gut dysbiosis and associated metabolome.

Suchitra Jena[1], Nikhil Bhalla[1], Shweta Chaudhary[1], Ranjan Kumar Nanda[1,*]

[1]Translational Health Group, International Centre for Genetic Engineering and Biotechnology, New Delhi component, New Delhi, 110067, India.

Running title: Microbiome dynamics in DM, TB and comorbid murine models.

*Corresponding author:

Ranjan Kumar Nanda (Ph.D.)

Translational Health Group,

International Centre for Genetic Engineering and Technology,

New Delhi-110067, India.

Telephone: 91-11-26741358

Email: ranjan@icgeb.res.in

Abstract:

Background: Diabetes and tuberculosis (DMTB) comorbid patients show atypical disease presentation and poor prognosis during treatment. In diabetes, the impaired immune system could partially be explained by the altered gut microbiota. Understanding gut microbiota and their association with the metabolite profiles in DMTB conditions may help design adjunct therapeutics.

Method: Nicotinamide (NA) and streptozotocin (STZ) induced diabetic C57BL/6 mice were aerosol infected with 100-120 CFU of *Mycobacterium tuberculosis H37Rv*. At different time points (2 days pre-infection and 3- and 8 weeks post infections; wpi), faecal samples were collected for microbiome and metabolome profiling using 16S rRNA sequencing and gas chromatography-time of flight-mass spectrometry (GC-TOF-MS), respectively.

Results: Diabetic mice showed gut dysbiosis, 16 bacterial genera were significantly altered between DMTB and TB at 3 wpi, which reduced to 11 at 8 wpi. Out of 93 identified faecal metabolites, a set of 11 and 10 deregulated ($\log_2 FC > \pm 1.0$, $p < 0.05$) metabolites were observed in the DMTB compared to TB groups at 3 and 8 wpi, respectively. Correlation analysis of microbiome and metabolome profiles showed a negative correlation between valeric acid levels in DMTB with the abundances of *Coriobacteriaceae, Granulicatella, Veillonella, Achromobacter, Erysipelatrichaceae, Atopobiaceae, Citrobacter,* and *Lactiplantibacillus*. Stronger metabolite-microbiota correlations were observed in DMTB comorbid conditions compared to TB. Correlation analysis also revealed phylogenetic distance-dependent synchrony in amino acid metabolism in five clades of 3 or more bacterial genera.

Conclusion: The present study highlights that the comprehensive landscape of gut microbiome and metabolome of DMTB are significantly different from TB. Certain microbes

and metabolic products could be useful as pre/probiotic concoctions for DMTB comorbid conditions for better recovery.

Keywords: Diabetes, Tuberculosis, Comorbidity, 16S rRNA sequencing, Metabolome, Microbiota, Metabolites, Valeric Acid, Clade-specific metabolic synchrony.

Introduction: Diabetes (DM) is a metabolic disorder characterised by high blood glucose levels, with an increase in case incidence from 200 million in 1990 to 830 million in 2022 (1, 2). DM patients show a higher susceptibility to infectious diseases like tuberculosis (TB), and present with severe symptoms and difficult to clinically manage. *Mycobacterium tuberculosis* (Mtb), the causative agent of TB, shows faster growth in the presence of sugar alcohols like glycerol in vitro. Diabetic patients with higher glycerol abundance probably facilitate faster Mtb growth, leading to a more severe form of TB (3). Due to different metabolic phenotypes, the DMTB and TB cases may present different disease pathologies, and detailed studies are missing.

The metabolic changes in diabetes cause low-level inflammation, higher oxidative stress, a compromised immune cell function and infiltration (4). DMTB subjects have relatively higher impairment in cell-mediated immunity and cytokine response, neutrophil inflammation, and alveolar macrophage responses. These factors contribute to higher morbidity in DMTB subjects, relapse rate and drug resistance development (5). The impact of DM on the digestive system, cause delayed gastric emptying in the upper gastrointestinal system and the small intestine, diabetes-associated enteropathy through vagal nerve dysfunction and negative impact on Cajal and nNOS interstitial cells (6–8). The slowed peristalsis in DM is often the cause of already-known small intestinal bacterial overgrowth, which can potentially affect the gut microbiota (6–8)

Gut microbiota plays a critical role in developing immunity in infants and preserving host health in adults by modulating the metabolism and immunological response. A healthy gut microbiota comprises six phyla: *Firmicutes*, *Bacteroidetes*, *Actinobacteria*, *Proteobacteria*, *Fusobacteria*, and *Verrucomicrobia* (10). DM associated gut dysbiosis leads to overgrowth of opportunistic pathogens belonging to *Bacteroides*, *Clostridium*, *Eggerthella*, and *Escherichia* (9). DM-induced gut dysbiosis is linked with impaired beta cell function, insulin sensitivity, and glucose metabolism (9–11). A decreased abundance of *Clostridiales* and a higher abundance of *Pophyromonodaceae* with treatment were reported in TB patients (12,13). Investigating the influence of diabetes in Mtb infected subjects on gut microbiota and associated metabolite profiles could be useful to better understand the disease aetiology.

In this study, a comparative faecal microbiota and metabolite profiling of DMTB and TB groups at various time points with their controls was attempted. The finding of the current study provides useful details in designing pre/probiotic concoctions of bacterial cultures and metabolites for DMTB comorbid conditions.

Results:

Diabetes induction and experimental plan to determine the impact of diabetes on the faecal metabolome and microbiome of Mtb-infected mice: The mice used in this study were the same as those described previously, with the detailed diabetes validation metrics (14). Briefly, a set of C57BL/6 male mice (8-12 weeks) received a nicotinamide-streptozotocin (NA-STZ) combination and developed hyperglycemia and dyslipidemia before aerosol infection with low dose (100-120 CFU) of Mtb H37Rv using a Madison Aerosol Chamber in BSL-III aerosol challenge facility at the host institute (Figure 1).

Gut microbiome dynamics are impacted by diabetes: To understand the microbiome dynamics in hyper and euglycemic mice at different time points, 16S rRNA sequencing was

performed (Figure 2A). The PCoA plot of euglycemic mice showed a time-dependent change but was minimal in DM mice (Figure 2B). The alpha diversity determined using Shannon's index was significantly higher in the DM than in healthy at week 3, and a time-dependent decrease in the variance in alpha diversity was observed (Figure 2C). To determine the microbes showing significant changes in their abundance, a multi-group analysis using one-tailed ANOVA was performed. It revealed time-specific perturbations in groups ($p < 0.05$), and 22 microbiota were down selected and further divided into five trend-specific clusters. Cluster-I, included *Dubosiella*, *Akkermansia* and *Erysipelatoclostridium*, which were lower in abundance in DM, while in healthy, their abundance decreased over time (Figure 2D). Cluster-II, included *Parvibacter*, *Parasutterella*, *Muribaculum*, *Family XIII UCG-001*, *Butyricicoccus* and *Olsenella*, which remained similar in DM, unlike the healthy (Figure 2E). Cluster-III, included *Serratia*, *Harryflintia*, *Deslfovibrio* and *Atopobiaceae*, and their abundance was lower in the DM group (Figure 2F). Cluster-IV included *Weissella*, *Limosilactobacillus*, *Lachnospiraceae UGC-0* and *Enterobacter*, and their abundance remained low in healthy but present in DM (Figure 2G). All genera in Cluster-V showed a unique pattern. *Alloprevotella* abundance was low in DM at both time points. UCG-010 showed inverse abundance patterns between the DM and the healthy group. DNF0089 showed a time-dependent increase in both the healthy and diabetes groups, with a slower rate in DM. *Odoribacter* showed a decrease in abundance at week 3, followed by a minor increase at week 8 in the DM group. In healthy. *Allobacculum* showed a stable abundance close to zero in the DM group, and a time dependent increase in trend was observed in healthy (Figure 2H). These findings demonstrate that the DM mice show a significant change in their microbial abundance over time, which could impact their microbiota-associated metabolic profiles.

Faecal metabolites are impacted by diabetes in Mtb infection: To understand DM-associated metabolite differences in Mtb-infected mice, we compared the faecal metabolites of DMTB and TB groups (Figure 3A). The rest of the comparative metabolite differences are presented in the supplementary (Figure S2). The PCA plot of DMTB and TB groups at 3 and 8 wpi showed partially overlapping clusters (Figure 3B and 3C). At 3 wpi, a set of 11 deregulated (3/8: up/down; $\log_2 FC > \pm 1.0$, students t-test $p < 0.05$) metabolites were observed in the DMTB compared to the TB group. Increased abundance of methyl-alpha-D-glucopyranoside, 2-hydroxyadipic acid, 4-methylmandelic acid, 2-hydroxyvaleric acid, L-leucine, L-tryptophan and sugars such as D-(-)-ribofuranose and D-xylopyranose and a lower abundance of pseudo uridine, pipecolinic acid, phosphoric acid was observed (Figure 3D). At 8 wpi, a set of 10 deregulated metabolites was identified, out of which abundance of L-tryptophan, GABA, 5-aminovaleric acid, D-pinitol, 5-hydroxyindole-3-acetic acid and xylulose were higher in DMTB than TB. In contrast, low abundance of L-leucine, pipecolonic acid, valeric acid and 3-hydroxyphenylpropionic acid was observed in the DMTB group (Figure 3E). At 3 wpi, pseudo uridine was significantly low in DMTB compared to TB, but at 8 wpi, it was lower. Higher L-tryptophan levels were observed in the DMTB group at both time points, indicating its association with diabetes. L-leucine in the DMTB group was higher at 3 wpi, and reduced at later time points, i.e. 8 wpi, compared to the TB group. At 3 wpi., the DMTB group showed higher 2-hydroxy adipic acid (2-HAA) abundance compared to TB and a similar trend was observed between DM and healthy (Figure S1D). Pipecolinic acid, phosphoric acid, pseudo uridine and D-pinitol decreased over time in the TB group. Decreased abundance of L-leucine and higher 5-amino valeric acid and L-tryptophan levels were observed in the DMTB group with time (Figure 3F). These results indicate that DM drives significant changes in the abundance of certain faecal metabolite levels. These observed changes could be contributed by the altered host and microbiota metabolisms.

Faecal microbiome of hyper and euglycemic mice alters upon Mtb infection: To determine the influence of diabetes upon Mtb infection, a comparative microbiome profiling between DMTB and TB was carried out at two-time points, i.e. 3 and 8 wpi. The microbiota of DMTB and TB groups clustered separately, indicating a significant difference in their beta diversity at 3 and 8 wpi (Figure 4A, 4B). The healthy controls were clustered away from the DM group but had similar beta diversity with healthy controls. The alpha diversity of the DM group showed a subtle and significant ($p<0.01$) increase compared to healthy controls (Figure 4C). Although the DMTB group showed a subtle ($p=0.06$) increase in alpha diversity from healthy control and was similar with TB. The TB group had lower alpha diversity than the DM group at 3 wpi. At 8 wpi, the differences in alpha diversity were insignificant between all study groups (Figure 4D).

To capture time-dependent changes in the microbiome profile of DMTB and TB groups, a pairwise analysis between 3 and 8 wpi were carried out. The abundance of *Allobaculum, Desulfovibrio, Ileibacterium* and *Eubacterium fissicatena group* was higher in the DMTB group. Similarly, an abundance of the *Clostridium innocuum group* and *Eschereichia-shigella* genera were observed to be low in the DMTB group compared to the TB group. Whereas we observed significant variations in bacterial genera, at 3 wpi, abundance of *Clostridium innocuum group, Prevotellaceae UGC-001, Odoribacter, Bacteroides, Monoglobus, Klebsiella, Weissella* and *Acinetobacter* were low and higher *Dubosiella, Bifidobacterium, Lachnospiraceae AC2044,* and also a family i.e. *Erysipelatoclostridiceae* (Figure 4E top right). At 8 wpi, a higher abundance of *Mucispirillum* and a lower abundance of *Ruminococcus* and *Eubacterium* groups was observed in DMTB (Figure 4E Bottom right). A multigroup analysis yielded similar findings observed in the pairwise analysis (Figures 4F and 4G, Supplementary Figure S2). These findings indicate that DM induced severe microbial gut dysbiosis in Mtb infected study group.

Microbiome-metabolite differential correlation analysis revealed phylogenetic distance-specific synchrony in amino acid metabolism of gut microbiota: Diabetic condition perturbs both the host microbiome and metabolic profile. We aimed to correlate the gut microbiome and the deregulated metabolome, if any, in the DMTB group and whether it is different from TB. Multiple correlation clusters were observed in the DMTB comorbid group compared to the TB (Figure 5A-D). L-tryptophan, which was higher in DMTB, showed positive correlations at 3 wpi with *Prevotellaceae, Succinivibrio, Acinetobacter, Faecalibacterium, Neisseria* and at 8 wpi with *Paludicola, Halomonas, Enterococcus, UCG-005, Rikenella*. A higher abundance of L-leucine at 3 wpi was positively correlated with *Anaerococcus, NK4A214 group,* and *Eubacterium coprostanoligenes group*. At 8 wpi, *Anaerococcus* (r=-0.16), *NK4A214 group* (-0.57) and *Eubacterium coprostanoligenes group* (r=-0.45) showed a negative correlation with L-leucine. Pipecolinic acid levels were low in DMTB, were negatively correlated (r=-0.7 or 7.0) with *Prevotellaceae, Roseburia, Escherichia-Shigella, HT002* and at 8 wpi correlated with *Ileibacterium, Anaerofilum, Erysipelotrichaceae* (Figure S3). Differential correlation analysis of microbiome-metabolome of DMTB comorbid and TB showed higher deregulated clusters at 3 wpi. *Atopobiaceae, Achromobacter, Anaerofilum, Citrobacter, Coriobacteriaceae UCG-002, Erysipelotrichaceae UCG-003, Granulicatella, Lactiplantibacillus, Veillonella* showed a negative correlation ($r<-0.9$, $p_{adj}<0.001$) with valeric acid in DMTB group compared to TB group at 3 wpi. *Christensenellaceae r-7 group* and *Lachnospiraceae AC2044* group negatively correlated ($r<-0.9$, $p_{adj}<0.001$) with citric acid in DMTB than in the TB group. *Anaerofilum* and *Lactiplantibacillus* negativly correlated ($r<-0.9$, $p_{adj}<0.001$) with d-(+)-ribono-1,4-lactone. This indicates that the metabolic states of bacteria from different genera are in higher metabolic synchrony in DMTB compared to the TB group (Figure 5B). At 8 wpi, *Porphyromonas*, and *Ruminiclostridium* positively correlated with L-norleucine ($r>0.6$,

p_{adj}<0.001), indicating their synchronised metabolic states (Figure 5C). In addition, a subset of amino acids and their derivatives showed correlations in DMTB at 8 wpi (Figure S3D). A filtered heat map of these amino acids showed 5 clusters, each consisting of 3 or more genera, correlated with amino acid levels (Figure 5G). These findings suggest substantial correlations between microbiome and metabolome in DMTB groups and possible synchrony in their metabolic states in a phylogenetic distance-dependent manner for selected genera.

Discussion: Diabetes cases are increasing significantly and are becoming a global concern. DM incidence rates in countries reported to have a direct impact on the human development index (15,16)**.** DM patients often show systemic metabolic changes in the body, higher levels of advanced glycation end products and chronic inflammation which increases susceptibility to infectious diseases like TB. DM subjects also produce lower IFN-γ and TNF-α levels, critical for controlling Mtb growth inside macrophages. The DMTB comorbid patients reported higher proinflammatory IL-1β, Il-6, and LI-18 cytokines and the macrophages, when exposed to high blood sugar levels, compromised their Mtb phagocytic ability. All these perturbed immune systems in DM result in poor prognosis and may affect Mtb dissemination, causing more severe miliary TB and contributing to drug resistance development (17).

Microbiota contributes to a stronger immune system development and prolonged or unnecessary use of antibiotics, diet change, or systemic constraints orchestrated by conditions like DM, and genetic factors like mutations in NOD2 (prevents gut inflammation) and ATG16L1 (aids in exocytosis in paneth cells) cause dysbiosis and negatively impacts the immune system. Dysbiosis in diseased states like inflammatory bowel disease leads to a decrease in alpha diversity, for example, lower *Ruminococcaceae* and *Lactobacillus* abundance and higher *Proteobacteria*. The intricate microbiota-immune system crosstalk in a diseased state can drive changes in Th17, Th2, and Th1 cell counts and decrease Treg and IgA

levels, further exacerbating the pathogenesis (18). Metabolites derived from microbes may act as conduits for the crosstalk between microbiota and the immune system. In diabetes, a leaky gut is commonly reported and contributes to generating autoantibodies, resulting in a higher systemic inflammation (19,20). Gut dysbiosis in DM and TB patients has already been reported. However, studies on DM-TB comorbid conditions are limited and need a better understanding (12,21,22).

In the present study, we focused on the metabolome and microbiome landscape of DMTB comorbidity and TB in murine models. Several genera of gut microbiota showed perturbations in their relative proportions in the DMTB group. A decreased alpha diversity in TB and DM patients, compared to healthy subjects, was reported in the literature (23–26). Few studies also reported non-significant changes in alpha diversity in DM patients, indicating the involvement of other factors, possibly be due to multiple experimental factors (27,28). In this study, an increase in alpha diversity was observed at one time point (i.e. 3 weeks) in the DM group. In DM patients and obese subjects, a lower abundance of *Akkermansia* was reported, and similar findings observed in this mice study (29). Corroborating with previous literature, we consistently observed altered beta diversity in the DM group (27). At the genus levels, *Allobaculum*, was low in the DM group, which has an intestinal protective role and a reduced abundance of it was reported in the insulin resistance cases (29). An increased abundance of *Allobaculum* was observed in DMTB compared to TB, which seems to be mediated by DM. Higher *Allobaculum* abundance in mice with diabetic nephropathy, was reported earlier (30). Genera such as *Desulfovibrio* and *Acinetobacter* are also reported positively associated with hyperglycemia observed in DM or gestational DM (31). *Desulfovibrio* is a sulphate-reducing genus that produces hydrogen sulfide, which contributes to an increase in inflammation (32,33). In the DMTB group, a higher abundance of *Desulfovibrio* was observed, suggesting the change is majorly contributed by diabetes. We

observed a higher abundance of *Acinetobacter* in the diseased states (DMTB/TB; DMTB/HC at 8 wpi and TB/HC, 3 wpi), corroborating earlier reports that showed diabetes as a risk factor for *Acinetobacter baumannii* infection (34,35).

Diabetes may impact the microbiome-associated metabolomic landscape. For example, pipecolinic acid, a lysine catabolism product that gut microbes produce, was lower in the DMTB group (36). A negative correlation of serum pipecolinic acid levels with high blood glucose levels in diabetic retinopathy patients and coronary artery disease-diabetic comorbid subjects has already been reported earlier (37,38). At 8 wpi low pipecolinic acid and *Ruminococcus* abundance were observed in the DMTB group compared to the TB group, highlighting their correlation. L-tryptophan was higher in the DMTB group, which gets converted to other secondary metabolites like tryptamine and indoles like indole-3-aldehyde, indole-3-acetic-acid and indole-3-propionic acid by the gut microbiota (39,40). The altered microbial diversity observed in the DMTB group might contribute to the observed higher tryptophan levels. Dysbiosis in DM leads to decreased levels of short chain fatty acids (SCFA)-producing gut bacteria and reduced SCFAs (viz., propionic acid, and butyric acid) (41). SCFAs provide protective functions like promoting anti-inflammatory effects and immune responses. The metabolite-microbiota correlation analysis showed a link between SCFA and valeric acid and the microbes that degrade lactate and produce SCFAs as its by-products, like *Coriobacteriaceae UGC-002*. *Coriobacteriaceae UGC-002*, belonging to the *Actinobacteria* phylum, is an SCFA-producing bacteria. *Coriobacteriaceae* is reported to be negatively correlated to hyperglycemia observed in diabetes, while it is positively correlated in TB (42–44). A negative correlation between valeric acid and *Coriobacteriaceae UGC-002* was observed between the DMTB and TB group at 3 wpi. The reduced valeric acid levels in TB with an increased *Coriobacteriaceae* level indicate its impact on DMTB comorbidity. In a recent report, the administration of probiotics in T2DM patients increased valeric acid levels,

and a similar correlation between valeric acid and similar probiotic bacteria was observed in this study (45).

Microbiota also demonstrates metabolic state synchrony by coordinating the gut microbiome and metabolism with circadian rhythm (46,47). We observed correlating amino acid levels and microbiota in a phylogenetic distance-specific manner, indicating possible synchrony in microbial metabolism for selected genera. Previous reports indicated that gut tryptophan metabolism affects the glycemic state through peripheral serotonin, impacting host homeostasis (48). Also, the involvement of intestinal microbiota in amino acid utilization for SCFA production and the impact of T2DM on it is well-known (49). Our findings highlight higher synchrony in amino acid metabolism in the DMTB group and shed light on phylogenetic clades that may have a role in SCFA production and intestine wall protection.

There are a few limitations in this study, including the use of male mice, a small sample size and the inherent differences in the DM murine model and its translational potential in patients. Further expansion using a larger sample size, including female mice and understanding the effect of TB drugs on the studied aspects will provide more meaningful information.

Conclusion: This study demonstrated specific gut microbiota dysbiosis and metabolic dysfunction in the DMTB comorbid condition compared to TB controls. Several gut microbes and associated metabolites were identified as DMTB markers and could be useful for developing therapeutic interventions in the form of pre/probiotic supplements.

Methodology:

Diabetes induction and Faecal matter collection: The animal experimental protocols in this study were approved by the animal ethics committee (vide reference ICGEB/IAEC/07032020/TH-13Ext) of the International Centre for Genetic Engineering and

Biotechnology New Delhi component. Faecal samples were collected from the mice used for another study (14). Briefly, male C57BL/6 mice aged 8-12 weeks were administered nicotinamide (60 mg/kg in 0.9% saline; NA) and 15 minutes later streptozotocin (150 mg/kg in 50 mM citric acid buffer; STZ) 3 times at an interval of 10 days each. To establish DM, blood glucose levels were monitored for several weeks after the last NA-STZ dose (14). Fresh faecal pellets (at least 2-3 per mouse) were collected in containers directly from the mice after gentle pressing and stored at -80°C until further processing.

Faecal metabolite extraction and derivatisation for GC-TOF-MS data acquisition and data processing: To the faecal samples (50 mg), zirconia beads (300 mL, 0.1 mm diameter), chilled methanol (80%, 1 mL) and ribitol (0.5 mg/mL, 2 mL) were added and subjected to bead-beating (3 cycles) using BioSpec Bead beater. The homogenised faecal sample was centrifuged at 16,000 g at 4 °C for 15 minutes, and the supernatant was harvested. A fraction of the extracted faecal metabolite (400 mL) was vacuum-dried using SpeedVac (Labconco, USA) at 40 °C for complete dryness to treat with methoxamine–hydrochloric acid mix (40 µL, MOX-HCl, 20 mg/mL) for 2hrs at 60 °C, 900 rpm. After that, the reaction mixture was incubated with N-methyl-N-(trimethylsilyl) trifluroacetamide (MSTFA, 80 mL) and trimethylchlorosilane (TMCS;1%) for 30 min at 60 °C at 900 rpm. After centrifugation at 16,000 g for 10 min at room temperature, the supernatant was harvested and transferred to GC vials for GC-TOF-MS acquisition.

GC-TOF-MS and data processing: Using an automated multipurpose sample introduction system, the derivatised samples were loaded into the column attached to the GC-TOF-MS instrument (Agilent Technologies, Santa Clara, CA) in split-less injection mode. Helium was used as a carrier gas with a 0.5 ml/min flow rate for each run. Metabolite separation was carried out in an RTX-5 column (30 m, 0.25 mm, 0.25 mm) with a temperature gradient from

60-300°C at a ramp rate of 10°C/min (60-220°C) and 5°C/min (220 to 300°C). Hold times of 1 min and 5 min were kept at the start and end of the run, respectively. The injection port temperature was held at 250°C throughout the run. Mass spectrometric data acquisition was carried out at -70 eV, and a mass range of 50-550 was scanned with a rate of 50 spectra per second. A 600-sec solvent delay was used as the GC-MS parameters and was controlled using ChromaTOF software (version 4.50.8.0; Leco, USA). Raw GC-MS data files (n=103), including all QC and study samples, were processed and aligned using the "Statistical Compare" feature of ChromaTOF. The minimum peak width was set at 1.3 sec for peak picking, and the signal-to-noise ratio (S/N) threshold was 75 for tentative molecular feature identification, mainlib, nist_ri, nist_msms2, nist_msms, and replib libraries from NIST were used. The maximum retention time difference was set at 0.5 sec, and the minimum spectral similarity was set at 600 for the spectral match. Aligned peak information was exported in ".csv" format, and molecules absent in more than 50% of samples of at least one class were excluded from the analysis. Before statistical analysis, manual data curation was carried out to align peaks and remove unsilylated molecules and silanes from the data matrix.

Total DNA extraction from faecal samples: The faecal sample (150-200 mg) were subjected to homogenisation through vortexing in 250 µL of $Tris_{50mM}EDTA_{1mM}$ buffer (pH 8.0) with 4 glass beads (2.7mm). The homogenates were treated with 50 µL of lysozyme (10 mg/mL), 50 µL of mutanolysin (3KU/mL) and 3 µL of lysostaphin (4KU/mL) for 1 hour at 37°C. 300 µL of 4 M guanidine thiocyanate (GITC) were added and mixed for 45 seconds. Next, 300 µL of 10 % N-lauryl sarcosine were added, incubated for 10 mins (300 rpm, 37°C), mixed and incubated (1hr, 70°C) followed by two cycles of bead beating (with 300mg of zirconia, 0.1 mm). Poly(vinylpolypyrrolidone) (PVPP, 15mg) was added and mixed, followed by centrifugation at (16,000 g, 3 mins). The supernatant was saved, and the pellet was washed twice with 500 µL of Tris(50mM)- EDTA(20mM)- NaCl(100mM)- PVPP(1%)

buffer, centrifuged, and the supernatant was pooled. The pooled supernatant was centrifuged (16,000g, 3 mins). To the resulting supernatant,4 mL of isopropanol was added and incubated at room temperature for 10 mins, followed by centrifugation (16,000g, 10 mins). The supernatant was discarded, and the pellet was dried for 1hr at 42°C. To the dried pellet, phosphate buffer and potassium acetate (1.0 mL, 9:1) were added and incubated overnight at -20°C. The samples were centrifuged (16,000g, 30 minutes, 4°C). RNase A (4 μL, 10 mg/mL) was added to the supernatant and incubated for 30 minutes at 37°C. To the supernatant, 100 μL of 3M sodium acetate was added, followed by the addition of ice-cold ethanol (96%), mixed, and subsequently incubated for 5 minutes at room temperature. The samples were centrifuged (16,000g, 15 minutes) at 4°C, and the pellet was washed with ice-cold ethanol (70%). The pellets were dried in an incubator for 1hr at 42°C. The dried pellets were then resuspended in 150 μL of nuclease-free water (NFW) and incubated for 10-15 mins at room temperature, followed by centrifugation at 16,000g for 10 mins at 4°C. The supernatant was stored and quantified using a Qubit 3.0 Fluorometer.

Enrichment of 16S rRNA and Sequencing: V3 and V4 regions of the 16S rRNA gene (rrS) gene were amplified using the following primers: *Forward Primer: 5'-TCGTCGGCAGCGT CAGATGTGTATAAGAGACAGCCTACGGGNGGCWGCAG-3 and Reverse primer: 5' GTCTC GTGGGCTCGGAGATGTGTATAAGAGACAGGACTACHVGGGTATCTAATCC-3'*. The amplification was done using KAPA high-fidelity polymerase. PCR products were purified and quantified using the Qubit dsDNA quantitation method (Invitrogen Inc, USA). For the preparation of the NGS library, the amplified DNA was subjected to Tagmentation using a NexteraXT kit (Illumina Inc, USA). Sequencing was carried out in the 300x2 paired-end configuration on the Illumina Novaseq platform (Illumina, USA).

Data processing: The sequencing reads were subjected to rigorous processing using NF-core/ampliseq pipeline v2.12.0v. NF-core/ampliseq pipeline included DADA2-based ASV

calling, and a taxonomy assignment was carried out. SILVA 138 database was used to annotate the amplicon sequence variants. The ASV matrix and taxonomy files were subsequently analysed using QIIME2 v2024.10.1. The analysis was done at the genus level. The ASVs that were unclassified at the genus level were summed up and studied at the family level.

Clustering of genera and molecules: For genera, the 16S rRNA sequences were extracted from the taxonomy file from DADA2 output and aligned with clustal omega and the Newick tree was calculated with FastTree. For metabolites, the SMILES were used to generate fingerprints, which were used to determine the distance between molecules. The Newick tree generated from these was used to cluster correlation matrices between metabolite and microbiota.

Statistics: The metabolite data were normalised to the peak areas of the internal standard (ribitol). A pseudocount of 1 was added before the $\log_2$ transformation, and the log-transformed matrices were used for PCA analysis. The paired student's t-test was performed for differential abundance, and metabolites that showed $\log_2 FC > \pm 1$ with raw $p < 0.05$ were considered statistically significant. For microbiome analysis, pairwise comparisons were done using the Deseq2 package, and ANOVA and Kruskal-Wallis tests were used for multi-group analysis. A pseudocount of 1 was added to Deseq2 normalised counts before log transformation of the microbiome ASV matrix. The signals were converted to Z-scores, and pairwise Pearson's correlation coefficient was computed. Fisher's Z-test was carried out using Python libraries: numpy, pandas, scipy.stats.norm for differential c correlation analysis. The results were parsed in MS-Excel 2016 home edition. The figures were created using Python and GraphPad Prism 8.4.

Contributions: SJ and RKN conceptualized the study. SJ performed animal handling, faecal material collection, sample processing, and data acquisition using mass spectrometry and gDNA isolation. NB and SJ analysed the data, prepared figures, and prepared the first draft of the manuscript.

Acknowledgements: SJ acknowledges a Junior Research Fellowship from UGC. NB is financially supported by a grant from the Department of Biotechnology (DBT), GoI (Grant ID: National Network Project of National Institute of Immunology, New Delhi-[40267]). SC is SPM fellow supported by CSIR. RKN acknowledges core support from the ICGEB New Delhi Component. Ms. Riya Ahmed and Mr. Anil Behera from the Translational Health Group, ICGEB, New Delhi component, are acknowledged for providing technical help during the study.

References:

1. Goyal R, Singhal M, Jialal I. Type 2 Diabetes. In: StatPearls [Internet]. Treasure Island (FL): StatPearls Publishing; 2025 [cited 2025 Feb 25]. Available from: http://www.ncbi.nlm.nih.gov/books/NBK513253/

2. NCD Risk Factor Collaboration (NCD-RisC). Worldwide trends in diabetes prevalence and treatment from 1990 to 2022: a pooled analysis of 1108 population-representative studies with 141 million participants. Lancet Lond Engl. 2024 Nov 23;404(10467):2077–93.

3. Martinez N, Smulan LJ, Jameson ML, Smith CM, Cavallo K, Bellerose M, et al. Glycerol contributes to tuberculosis susceptibility in male mice with type 2 diabetes. Nat Commun. 2023 Sep 20;14(1):5840.

4. Daryabor G, Atashzar MR, Kabelitz D, Meri S, Kalantar K. The Effects of Type 2 Diabetes Mellitus on Organ Metabolism and the Immune System. Front Immunol. 2020;11:1582.

5. Prada-Medina CA, Fukutani KF, Pavan Kumar N, Gil-Santana L, Babu S, Lichtenstein F, et al. Systems Immunology of Diabetes-Tuberculosis Comorbidity Reveals Signatures of Disease Complications. Sci Rep. 2017 May 17;7(1):1999.

6. Lysy J, Israeli E, Goldin E. The prevalence of chronic diarrhea among diabetic patients. Am J Gastroenterol. 1999 Aug;94(8):2165–70.

7. Marathe CS, Rayner CK, Wu T, Jones KL, Horowitz M. Gastrointestinal Disorders in Diabetes. In: Feingold KR, Anawalt B, Blackman MR, Boyce A, Chrousos G, Corpas E, et al., editors. Endotext [Internet]. South Dartmouth (MA): MDText.com, Inc.; 2000 [cited 2025 Feb 20]. Available from: http://www.ncbi.nlm.nih.gov/books/NBK553219/

8. Sommers T, Mitsuhashi S, Singh P, Hirsch W, Katon J, Ballou S, et al. Prevalence of Chronic Constipation and Chronic Diarrhea in Diabetic Individuals in the United States. Am J Gastroenterol. 2019 Jan;114(1):135–42.

9. Qin J, Li Y, Cai Z, Li S, Zhu J, Zhang F, et al. A metagenome-wide association study of gut microbiota in type 2 diabetes. Nature. 2012 Oct;490(7418):55–60.

10. Carey IM, Critchley JA, DeWilde S, Harris T, Hosking FJ, Cook DG. Risk of Infection in Type 1 and Type 2 Diabetes Compared With the General Population: A Matched Cohort Study. Diabetes Care. 2018 Mar;41(3):513–21.

11. Ngo MD, Bartlett S, Ronacher K. Diabetes-Associated Susceptibility to Tuberculosis: Contribution of Hyperglycemia vs. Dyslipidemia. Microorganisms. 2021 Nov 2;9(11):2282.

12. Cao D, Liu W, Lyu N, Li B, Song W, Yang Y, et al. Gut Mycobiota Dysbiosis in Pulmonary Tuberculosis Patients Undergoing Anti-Tuberculosis Treatment. Microbiol Spectr. 9(3):e00615-21.

13. Diallo D, Somboro AM, Diabate S, Baya B, Kone A, Sarro YS, et al. Antituberculosis Therapy and Gut Microbiota: Review of Potential Host Microbiota Directed-Therapies. Front Cell Infect Microbiol. 2021 Dec 7;11:673100.

14. Chaudhary S, Sravya M, Pahwa F, V S, Singh P, Chaturvedi S, et al. Diabetes-Tuberculosis Comorbidity Characterized by Reduced Type-II Interferon and Elevated Th17 Responses [Internet]. bioRxiv; 2024 [cited 2025 Mar 3]. p. 2024.10.24.619799. Available from: https://www.biorxiv.org/content/10.1101/2024.10.24.619799v1

15. Ranasinghe P, Jayawardena R, Gamage N, Sivanandam N, Misra A. Prevalence and trends of the diabetes epidemic in urban and rural India: A pooled systematic review and meta-analysis of 1.7 million adults. Ann Epidemiol. 2021 Jun 1;58:128–48.

16. Alinaghian SA, Hamidzadeh S, Badrizadeh A, Khazaei Z, Souri A, Momenabadi V, et al. Burden of type 2 diabetes and its relationship with human development index in Asian countries: Global Burden of Disease Study in 2019. BMC Public Health. 2025 Jan 31;25(1):402.

17. Boadu AA, Yeboah-Manu M, Osei-Wusu S, Yeboah-Manu D. Tuberculosis and diabetes mellitus: The complexity of the comorbid interactions. Int J Infect Dis. 2024 Sep 1;146:107140.

18. Zheng D, Liwinski T, Elinav E. Interaction between microbiota and immunity in health and disease. Cell Res. 2020 Jun;30(6):492–506.

19. Sharma S, Tripathi P. Gut microbiome and type 2 diabetes: where we are and where to go? J Nutr Biochem. 2019 Jan 1;63:101–8.

20. Sadagopan A, Mahmoud A, Begg M, Tarhuni M, Fotso M, Gonzalez NA, et al. Understanding the Role of the Gut Microbiome in Diabetes and Therapeutics Targeting Leaky Gut: A Systematic Review. Cureus. 15(7):e41559.

21. Al Bataineh MT, Künstner A, Dash NR, Alsafar HS, Ragab M, Schmelter F, et al. Uncovering the relationship between gut microbial dysbiosis, metabolomics, and dietary intake in type 2 diabetes mellitus and in healthy volunteers: a multi-omics analysis. Sci Rep. 2023 Oct 20;13(1):17943.

22. Hu Y, Yang Q, Liu B, Dong J, Sun L, Zhu Y, et al. Gut microbiota associated with pulmonary tuberculosis and dysbiosis caused by anti-tuberculosis drugs. J Infect. 2019 Apr;78(4):317–22.

23. Maskarinec G, Raquinio P, Kristal BS, Setiawan VW, Wilkens LR, Franke AA, et al. The gut microbiome and type 2 diabetes status in the Multiethnic Cohort. PLoS ONE. 2021 Jun 23;16(6):e0250855.

24. Meiring S, van Baar ACG, Sørensen N, Holleman F, Soeters MR, Nieuwdorp M, et al. A Changed Gut Microbiota Diversity Is Associated With Metabolic Improvements After Duodenal Mucosal Resurfacing With Glucagon-Like-Peptide-1 Receptor Agonist in Type 2 Diabetes in a Pilot Study. Front Clin Diabetes Healthc. 2022 Jul 5;3:856661.

25. Khan R, Sharma A, Ravikumar R, Sivaprasad S, Raman R. Correlation of gut microbial diversity to sight-threatening diabetic retinopathy. BMC Microbiol. 2024 Sep 13;24(1):342.

26. Analysis of gut microbiota of obese individuals with type 2 diabetes and healthy individuals | PLOS One [Internet]. [cited 2025 Mar 3]. Available from: https://journals.plos.org/plosone/article?id=10.1371/journal.pone.0226372

27. Que Y, Cao M, He J, Zhang Q, Chen Q, Yan C, et al. Gut Bacterial Characteristics of Patients With Type 2 Diabetes Mellitus and the Application Potential. Front Immunol [Internet]. 2021 Aug 12 [cited 2025 Mar 3];12. Available from: https://www.frontiersin.org/journals/immunology/articles/10.3389/fimmu.2021.722206/full

28. Kitten AK, Ryan L, Lee GC, Flores BE, Reveles KR. Gut microbiome differences among Mexican Americans with and without type 2 diabetes mellitus. PLoS ONE. 2021 May 13;16(5):e0251245.

29. Zhang Y, Liu R, Chen Y, Cao Z, Liu C, Bao R, et al. Akkermansia muciniphila supplementation in patients with overweight/obese type 2 diabetes: Efficacy depends on its baseline levels in the gut. Cell Metab. 2025 Mar 4;37(3):592-605.e6.

30. Wang J, Ke W, Bao R, Hu X, Chen F. Beneficial effects of ginger Zingiber officinale Roscoe on obesity and metabolic syndrome: a review. Ann N Y Acad Sci. 2017 Jun;1398(1):83–98.

31. Li Y, Su X, Gao Y, Lv C, Gao Z, Liu Y, et al. The potential role of the gut microbiota in modulating renal function in experimental diabetic nephropathy murine models

established in same environment. Biochim Biophys Acta Mol Basis Dis. 2020 Jun 1;1866(6):165764.

32. Dias S, Pheiffer C, Adam S. The Maternal Microbiome and Gestational Diabetes Mellitus: Cause and Effect. Microorganisms. 2023 Aug 31;11(9):2217.

33. Singh SB, Carroll-Portillo A, Lin HC. Desulfovibrio in the Gut: The Enemy within? Microorganisms. 2023 Jul 7;11(7):1772.

34. Dordević D, Jančíková S, Vítězová M, Kushkevych I. Hydrogen sulfide toxicity in the gut environment: Meta-analysis of sulfate-reducing and lactic acid bacteria in inflammatory processes. J Adv Res. 2021 Jan 1;27:55–69.

35. Leung CH, Liu CP. Diabetic status and the relationship of blood glucose to mortality in adults with carbapenem-resistant Acinetobacter baumannii complex bacteremia. J Microbiol Immunol Infect Wei Mian Yu Gan Ran Za Zhi. 2019 Aug;52(4):654–62.

36. Luo G, Spellberg B, Gebremariam T, Bolaris M, Lee H, Fu Y, et al. Diabetic murine models for Acinetobacter baumannii infection. J Antimicrob Chemother. 2012 Jun;67(6):1439–45.

37. Fujita T, Hada T, Higashino K. Origin of D- and L-pipecolic acid in human physiological fluids: a study of the catabolic mechanism to pipecolic acid using the lysine loading test. Clin Chim Acta Int J Clin Chem. 1999 Sep;287(1–2):145–56.

38. Liu Y, Liu JE, He H, Qin M, Lei H, Meng J, et al. Characterizing the metabolic divide: distinctive metabolites differentiating CAD-T2DM from CAD patients. Cardiovasc Diabetol. 2024 Jan 6;23(1):14.

39. Luo L, Cai Y, Jiang Y, Gong Y, Cai C, Lai D, et al. Pipecolic acid mitigates ferroptosis in diabetic retinopathy by regulating GPX4-YAP signaling. Biomed Pharmacother Biomedecine Pharmacother. 2023 Dec 31;169:115895.

40. Gao J, Yang T, Song B, Ma X, Ma Y, Lin X, et al. Abnormal tryptophan catabolism in diabetes mellitus and its complications: Opportunities and challenges. Biomed Pharmacother Biomedecine Pharmacother. 2023 Oct;166:115395.

41. Xie Y, Li X, Meng Q, Li J, Wang X, Zhu L, et al. Interplay between gut microbiota and tryptophan metabolism in type 2 diabetic mice treated with metformin. Microbiol Spectr. 2024 Oct 3;12(10):e0029124.

42. Zhang S, Cai Y, Meng C, Ding X, Huang J, Luo X, et al. The role of the microbiome in diabetes mellitus. Diabetes Res Clin Pract. 2021 Feb;172:108645.

43. Karlsson FH, Tremaroli V, Nookaew I, Bergström G, Behre CJ, Fagerberg B, et al. Gut metagenome in European women with normal, impaired and diabetic glucose control. Nature. 2013 Jun 6;498(7452):99–103.

44. Wang Y, Luo X, Mao X, Tao Y, Ran X, Zhao H, et al. Gut microbiome analysis of type 2 diabetic patients from the Chinese minority ethnic groups the Uygurs and Kazaks. PloS One. 2017;12(3):e0172774.

45. Ding X, Zhou J, Chai Y, Yan Z, Liu X, Dong Y, et al. A metagenomic study of the gut microbiome in PTB'S disease. Microbes Infect. 2022 Mar;24(2):104893.

46. Min Q, Wang Y, Jin T, Zhu L, Wu X, Li Y, et al. Analysis of Intestinal Short-Chain Fatty Acid Metabolism Profile After Probiotics and GLP-1 Treatment for Type 2 Diabetes Mellitus. Front Endocrinol. 2022 Jun 30;13:892127.

47. Zhao E, Tait C, Minacapelli CD, Catalano C, Rustgi VK. Circadian Rhythms, the Gut Microbiome, and Metabolic Disorders. Gastro Hep Adv. 2022 Jan 1;1(1):93–105.

48. Gutierrez Lopez DE, Lashinger LM, Weinstock GM, Bray MS. Circadian rhythms and the gut microbiome synchronize the host's metabolic response to diet. Cell Metab. 2021 May 4;33(5):873–87.

49. Li TT, Chen X, Huo D, Arifuzzaman M, Qiao S, Jin WB, et al. Microbiota metabolism of intestinal amino acids impacts host nutrient homeostasis and physiology. Cell Host Microbe. 2024 May 8;32(5):661-675.e10.

50. Neis EPJG, Dejong CHC, Rensen SS. The Role of Microbial Amino Acid Metabolism in Host Metabolism. Nutrients. 2015 Apr 16;7(4):2930–46.

Summary figure/ graphical abstract:

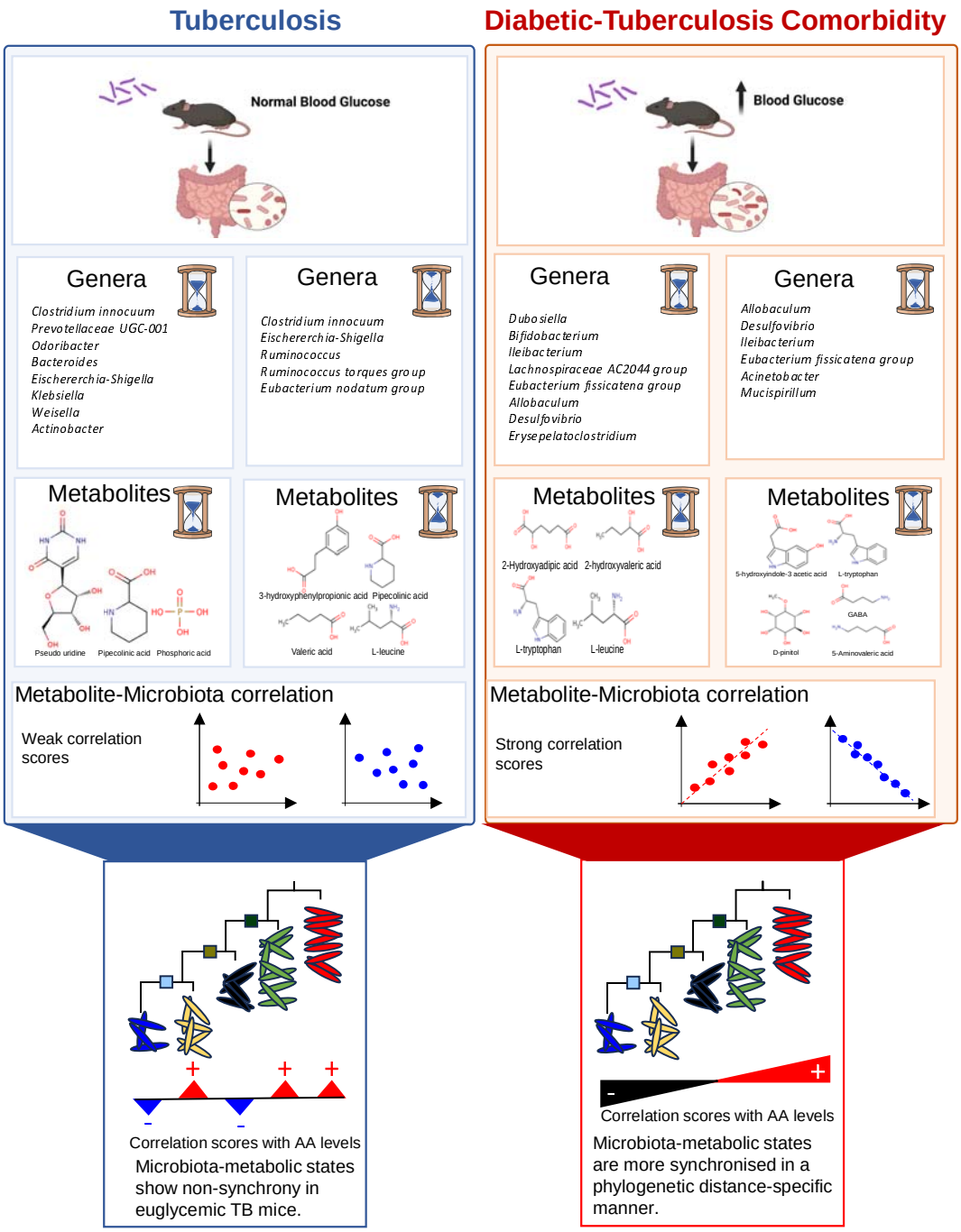

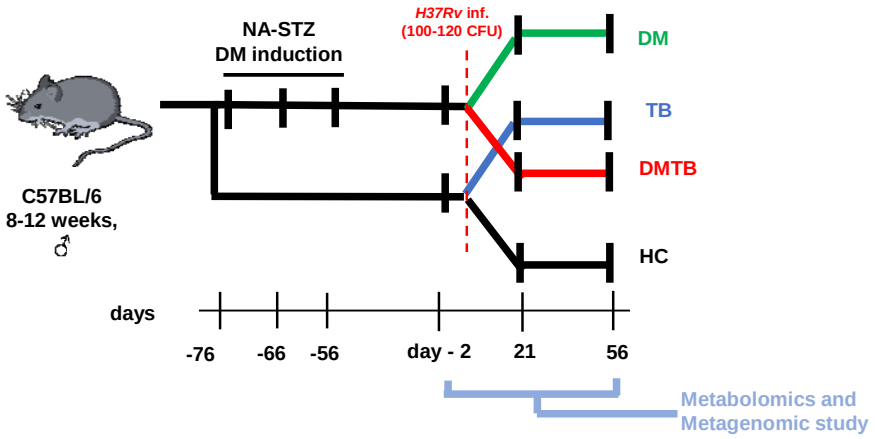

Figure 1: Experimental plan adopted in this study. Diabetic induction in C57BL/6 male mice (8-12 weeks old) was done using the nicotinamide-streptozotocin (NA-STZ) combination. Diabetes was confirmed with consistently elevated blood glucose levels after the last NA-STZ cocktail dose. A faecal sample was collected 2 days before and 3 and 8 weeks after Mtb infection. The infection was carried out through aerosol mode. Note: The mice used in this study were the same as those described previously, and diabetes validation can be found in our earlier published work (14). DM: diabetic, TB: Mtb infected, DMTB: Diabetic and Mtb infected (comorbid), HC: Healthy controls, NA: Nicotinamide, STZ: Streptozotocin, C57BL/6: mice strain.

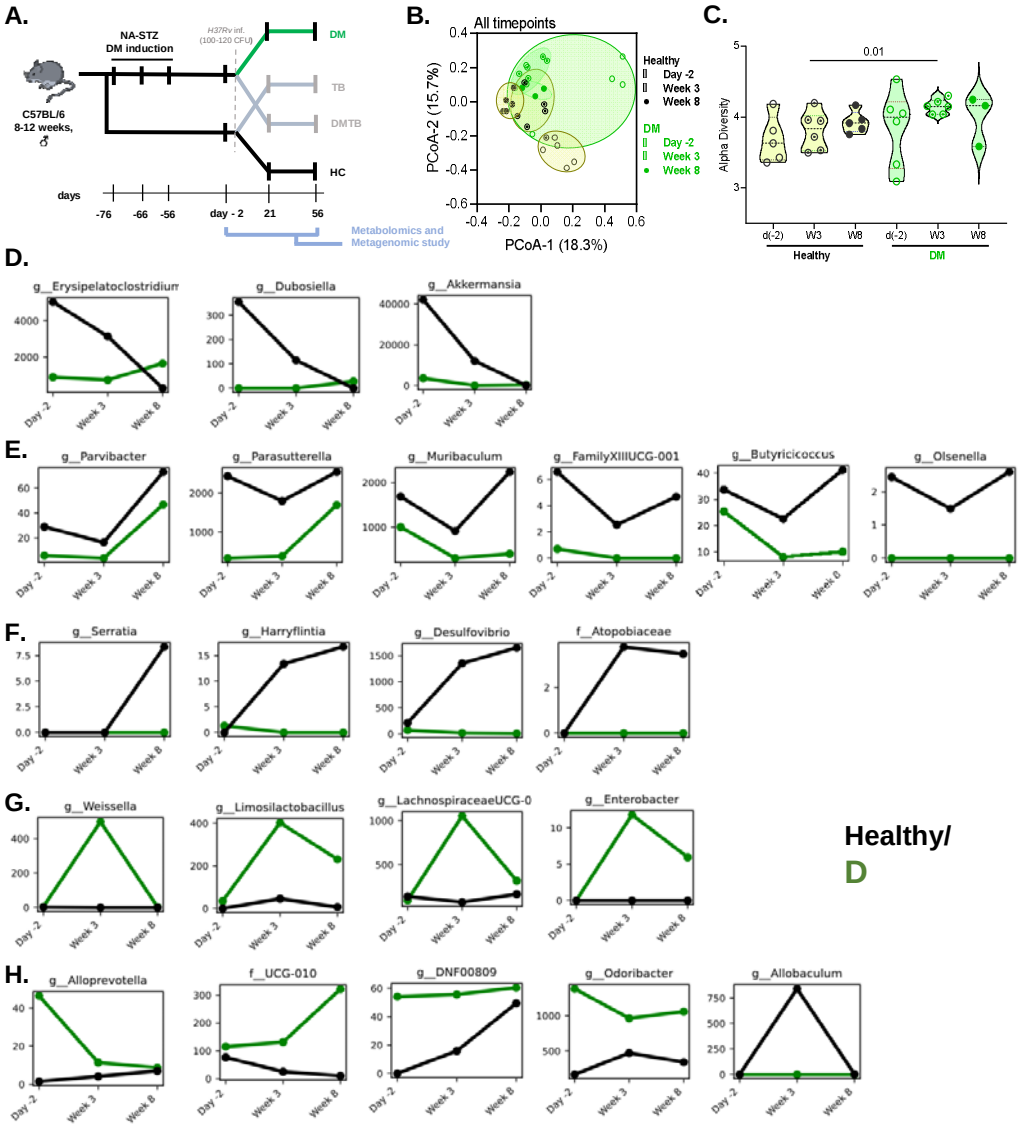

Figure 2: Faecal microbiome changes are impacted by diabetes. Diabetes was induced using an NA-STZ, and faecal matter was collected at three-time points. 16S rRNA sequencing of the faecal sample was performed as mentioned in the methodology, and Deseq2 normalized abundances were used for each genus group-wise and microbiome differences at different time points. Species that showed $p<0.05$ (One-way ANOVA) were down-selected, and their abundances were averaged for plotting against time points. A: PCA plot. B: Genera showed a decline after Mtb infection in healthy mice. C: miscellaneous trend observed. D: Genera showed a decrease at week 3 and an increase at week 8 after Mtb infection in Healthy with a similar but less pronounced effect in DM mice. E: Bacteria showed an increase only in healthy mice. F: Genera showed a sudden spike in week 3 and a sudden decrease in week 8 after the Mtb infection. G: Miscellaneous trend group 2. g: genus; f: family, DM: diabetic, TB: Mtb infected, DMTB: Diabetic and Mtb infected (comorbid), HC: Healthy controls, NA: Nicotinamide, STZ: Streptozotocin, C57BL/6: mice strain.

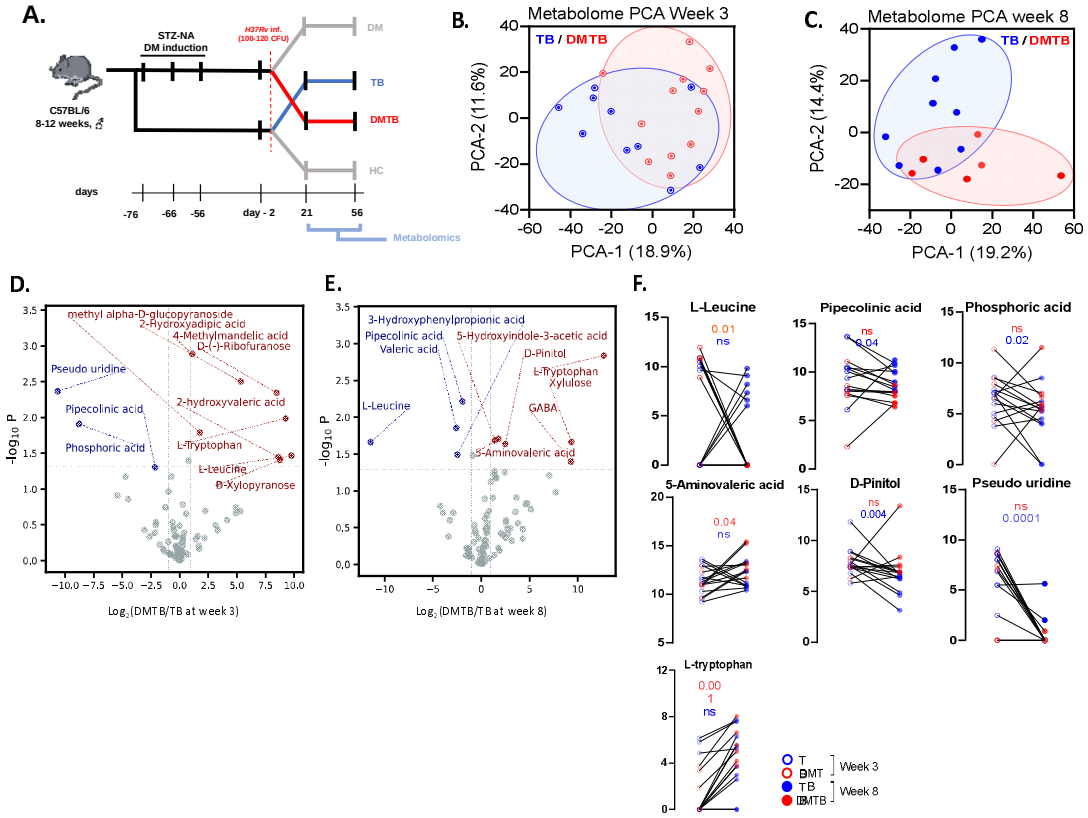

Figure 3. Metabolites are impacted by diabetes in Mtb infected mice. The metabolome matrix was normalized to the internal standard and log-transformed before being subjected to PCA and subsequently analyzed. A: Schematic representation of the experimental plan. B; C: PCA plot showing the clustering of the faecal metabolites at week 3 and week 8, respectively. D; E: Differential abundance analysis of metabolites of DMTB vs TB at weeks 3 and 8 post-Mtb infection. F: Levels of deregulated molecules in DMTB vs TB comparisons at weeks 3 and 8 (L-leucine, pipecolinic acid, phosphoric acid, pseudouridine 5-amino valeric acid, D-pinitol, and L-tryptophan). DM: diabetic, TB: Mtb infected, DMTB: Diabetic and Mtb infected (comorbid), HC: Healthy controls, NA: Nicotinamide, STZ: Streptozotocin, C57BL/6: mice strain, PCA: Principal Component Analysis, P: p-value.

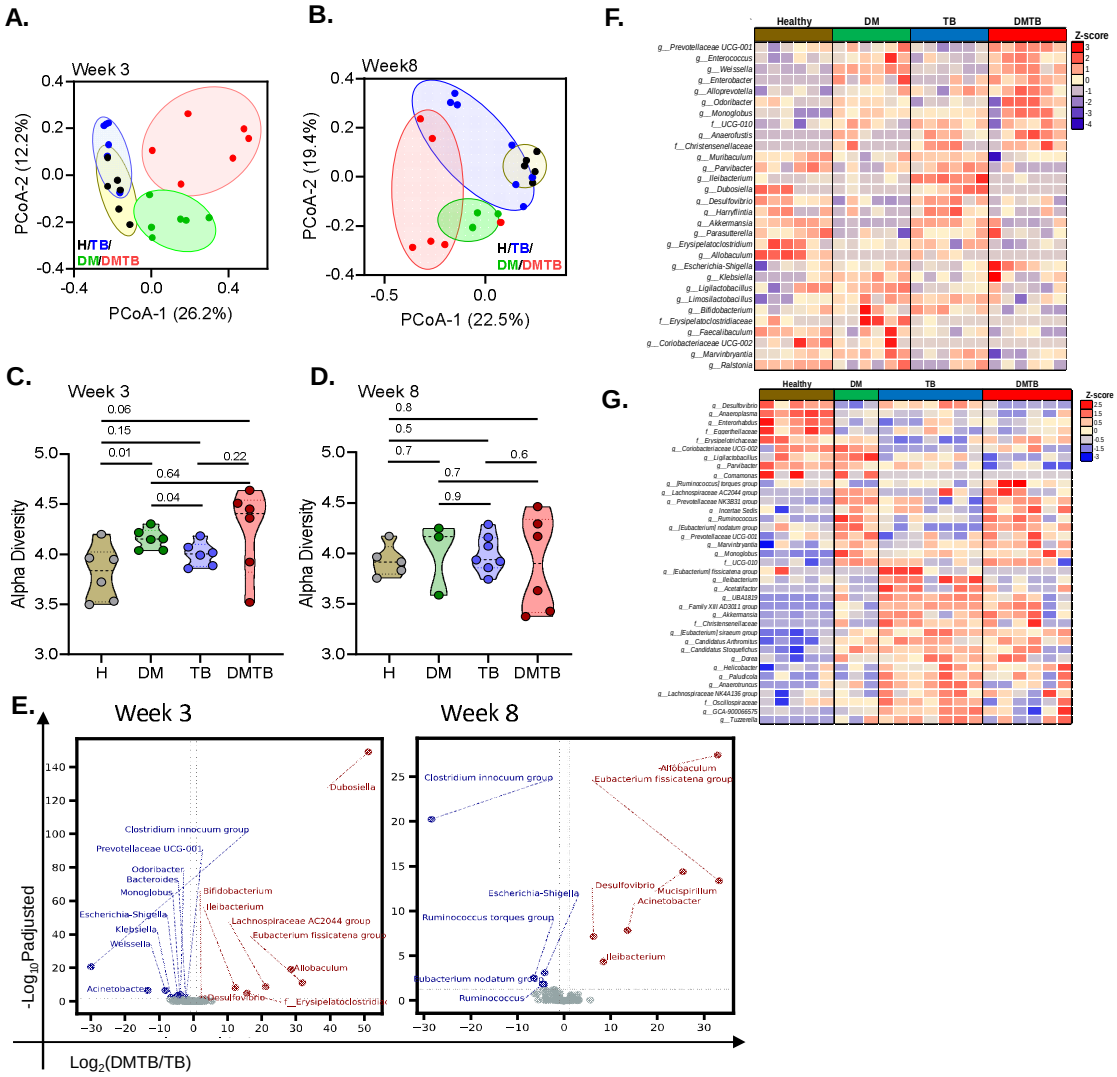

Figure 4. Faecal microbiome changes are impacted by diabetes after Mtb infection. Diabetes was induced in mice using the NA-STZ method and faecal gDNA isolated at 3 and 8 weeks post Mtb aerosol challenge were used for microbiome analysis by using 16S rRNA V3 and V4 specific primers. The sequencing library was prepared using a Tagmentation-based method, and 300x2 PE Illumina chemistry was used for sequencing. The sequencing data was subjected to NF-core/ampliseq standardized pipeline. DADA2 computed ASV matrix was normalized using edgeR for PCA analysis, and normalization was done with Deseq2 to determine microbes undergoing dysbiosis. A: PCoA plot at 3 weeks. B: PCoA plot at 8 weeks (Braycurtis Index). C: Alpha diversity at 3 weeks. D: Alpha diversity at 8 weeks (Shannon). E: Differentially abundant genera between DMTB and DM and TB at week 3 and week 8 post-infection. F and G: The Deseq2 normalized data converted to the first log2-transformed matrix, and species absent in 1/3rd of the samples were excluded from the analysis. Finally, the Kruskal-Wallis test was applied to each species to assess statistical significance across the groups (Healthy, DM, TB and DMTB). Species that showed p_{adj}<0.05 have been shown for week 3 and week 8 post Mtb infection. DM: diabetic, TB: Mtb infected, DMTB: Diabetic and Mtb infected (comorbid), HC: Healthy controls, NA: Nicotinamide, STZ: Streptozotocin, C57BL/6: mice strain, PCA: Principal Component Analysis, P: p-value.

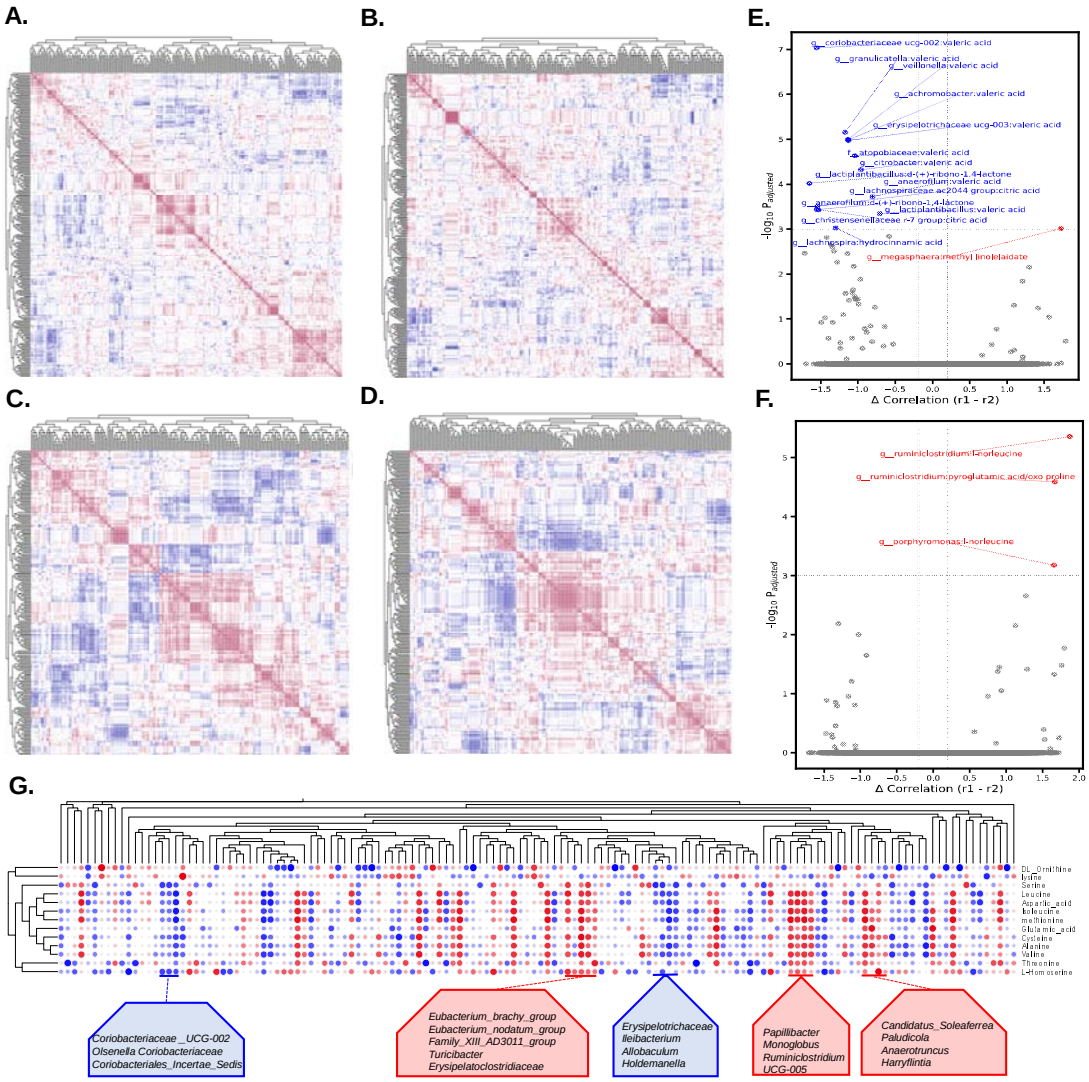

Figure 5: Metabolite-microbiome correlation analysis revealed a higher correlation in the DMTB group and phylo-distance specific metabolic synchrony in amino acid metabolism in some genera. A; B; C; D: Deseq2 normalized abundance and metabolite abundances were log-transformed and converted to Z-scores for correlation analysis within and between the microbiome and metabolome. The pairwise Pearson correlation coefficient between microbiome and metabolome was computed for DMTB and TB in weeks 3 and 8 post-Mtb infection. Correlation between microbes and metabolites is represented in the form of heatmaps at TB at week 3 (A), week 8 (B), DMTB at week 3 (C) and week 8 (D). E; F: Differential correlation analysis using Fisher's Z-test. The correlation differences with p_{adj} <0.0001 were considered significant. Differential correlation analysis between DMTB and TB at week 3 (E) and week 8 (F). G: Filtered correlation matrix showing clusters of bacteria with similar correlation with amino acids indicating metabolic synchrony. Note: If r1 - r2 > 0, the correlation is more positive in DMTB than in TB, and if r1 - r2 < 0, the correlation is more negative in DMTB than in TB. Abbreviations: r1: correlation coefficient in DMTB; r2: correlation coefficient in TB.